This is the accepted version of the article

Switchable Photovoltaic Window for On-Demand Shading and Electricity Generation

Published in

Solar Energy, Elsevier

Volume 232, 15 January 2022, Pages 433-443

https://doi.org/10.1016/j.solener.2021.12.071

Switchable Photovoltaic Window for On-Demand Shading and Electricity Generation

Maximilian Götz-Köhler[1,*] Udayan Banik[1], Hosni Meddeb[1], Nils Neugebohrn[1], Dennis Berends[1], Kai Gehrke[1], Martin Vehse[1] and Carsten Agert[1]

[1]German Aerospace Center (DLR) Institute of Networked Energy Systems, Carl-von-Ossietzky-Str. 15, 26129 Oldenburg Germany

*Correspondence: maximilian.goetz@dlr.de

SUMMARY

A next step in the development of transparent photovoltaic windows would be to introduce a switching mechanism that allows the user to switch the window between a transparent and an opaque state as desired to generate electricity and shade the building interior. In this work, we investigate a switchable photovoltaic window consisting of the combination of a semitransparent germanium solar cell and a gasochromic switchable magnesium mirror in a double glazing. We analyze the average visible transmittance (AVT) and spectral emissivity (ε) of the device in the transparent (AVT=18%, ε=0.27) and light harvesting states (AVT= 1%, ε=0.06). The thermal and electrical performance of the switchable solar cell is studied under varied solar irradiance. The experimental results are used to model the annual electricity generation of a switchable photovoltaic window in different climate regions under different switching scenarios, based on datasets from the Photovoltaic Geographical Information System (PV-GIS). The model suggests that especially in Mediterranean regions, switchable transparent photovoltaic windows with an efficiency of 2% can be a promising step to combine on-demand shading with electricity generation. Moreover, it shows that to generate more than 20 kWh/m² of electricity per year with this technology, the switching must be additionally coupled to the occupancy of the indoor spaces. Our model is applicable to other switchable PV technologies for evaluation purposes and to estimate ideal use cases.

Keywords

Switchable Solar Cell, PV Potential, Solar Windows, Semi-Transparent Solar Cell, Smart Shading, PV-GIS

1. INTRODUCTION

Semi-transparent photovoltaics (STPV) have become an important field of research and technological development. The combination of glazing elements with solar cells to create energy harvesting windows is a promising addition to building integrated photovoltaics (BIPV) (Lee et al., 2020; Traverse et al., 2017). Especially for tall buildings with large window-to-wall ratio (WWR) the area for rooftop and façade integrated PV is rather small, making the glass façade the dominant area for electricity generation from photovoltaic windows. Furthermore, these devices can eliminate the need for additional shading elements and improve the thermal comfort within a building (Asfour, 2018; Fung and Yang, 2008)

However, any STPV approach is always a compromise between power conversion efficiency and transparency to visible light (Lunt, 2012). A promising approach to overcome this limitation is the use of switchable transparent photovoltaic (SwTPV) windows. SwTPV windows could surpass static STPV in functionality by dynamically adjusting the transparency of the window to the outdoor conditions (Ke et al., 2019). While in light harvesting (LH) state, the solar device shows high absorption of light and generates electricity. In the light transmission (LT) state of the SwTPV, the absorption and electricity generation are reduced. The window would allow for dynamic shading of rooms by reducing and increasing the transparency on demand and generate electricity at the same time. It was shown recently that an office building in Australia equipped with dye-sensitized solar cells with electrochromic switchable transparency is capable of reaching annual energy savings of up to 32% (Fiorito et al., 2020). Other studies from different research groups characterize the change in cooling load and electricity

consumption of buildings with either electrochromic switchable windows (Dussault and Gosselin, 2017) or transparent thin-film PV (Liao and Xu, 2015; Martín-Chivelet et al., 2018; Peng et al., 2016; Peng et al., 2015; Skandalos and Karamanis, 2016).

Several different approaches to realize SwTPV devices have been studied by researchers in the recent years. Photovoltachromic devices which combine STPV with electrochromic layers are able to adjust their transparency to the incoming solar irradiation. The photovoltaic layers are used to power the electrochromic switching depending on the illumination intensity (Cannavale et al., 2014; Ling et al., 2021; Wu et al., 2009). Similar approaches also exist using polymer dispersed liquid crystal switchable layers (Murray et al., 2017). A different type of SwTPV device uses the thermochromic dissociation processes in perovskite solar cells (Lin et al., 2018; Wheeler et al., 2017). Furthermore, a photochromic dye sensitized solar cell was studied by Huaulmé in 2020 which changes from a transparent to an absorptive state during irradiation with photons (Huaulmé et al., 2020). While these devices were able to provide net energy for consumption, their switching is always coupled to the momentary irradiations. SwTPVs that can be actively switched by the user between LT and LH state would further increase the flexibility to adjust the device. This type of SwTPV was demonstrated with gasochromic switchable layers in combination with organic (Yao et al., 2020) and inorganic thin film PV (Götz et al., 2020a).

In this publication we model the power generation of a gasochromic SwTPV window in different regions of the world based on satellite global irradiance data from the European Commission's Photovoltaic Geographical Information System (PV-GIS) database (Huld et al., 2012; Šúri et al., 2005). We fabricate an inorganic SwTPV device in a double-glazing configuration and characterize its optical, electrical and thermal properties to improve the accuracy of the simulation. A model for the electricity generation of the SwTPV was prepared, which considers the climatic conditions of the deployment site, the hourly solar radiation, a switching scenario and technological aspects such as average visible transmittance, power conversion efficiency and thermal behavior. This work focusses on realistic switching scenarios describing the smart electricity generation in residential or commercial buildings depending on the

climatic region and the cardinal orientation. Our results show that switchable photovoltaic windows can be used in double glazing systems and have the potential to be integrated into buildings for smart shading and electricity generation.

2. EXPERIMENTAL PROCEDURES

2.1 Device functionality

The solar cell studied in this work consists of an ultra-thin amorphous germanium absorber sandwiched between an amorphous p-doped silicon layer and an n-doped microcrystalline silicon layer. The total thickness is kept below 40 nm to guarantee high transparency. The electrical front contact is aluminum doped zinc-oxide (ZnO:Al) which has also high transparency and high conductivity for charge carrier extraction. The back electrode of the solar cell introduces also the switchability of the system. A gasochromic magnesium layer allows the extraction of charge carriers and is able to change its reflectivity and transparency through the absorption of hydrogen diluted in a carrier gas. The detailed concept of this cavity enhanced solar cell and the functionality of the device is shown elsewhere (Götz-Köhler et al., 2021). The system of front contact, p-i-n cell and optically switchable electrode constitute an optical cavity which leads to absorption enhancement of light while the Mg layer is in its metallic state (Götz et al., 2020a; Steenhoff et al., 2015). The layer configuration can be seen in Figure 1a. In the as deposited state, the solar cell is in LH mode and almost completely opaque. After exposure to hydrogen gas, the Mg layer becomes transparent and the solar cell switches to LT mode. The switching takes ten minutes and is done with 5% H_2 diluted in N_2. The switching back into the LH state is done by exposure to ambient air for ten minutes.

2.2 Fabrication of switchable photovoltaic window

The transparent solar cells were fabricated on borosilicate glass. The glass was coated with 1000 nm ZnO:Al by PVD in a sputter facility (Vistaris 600, Singulus, Germany). The layer had a resistivity of $8 \cdot 10^{-3}$ Ωcm, measured in a 4-point probe configuration (Jandel, UK). On top of the ZnO:Al layer the n-i-

p layer structure was deposited as a-Si:H (p) / a-Si:H (i) / a-Ge:H (i) / µc-Si (i) / µc-Si (n) by PECVD (Leybold, Germany). The layer thicknesses are 7 nm / 5 nm / 5 nm / 5 nm / 7 nm. Detailed deposition parameters can be found in other publication (Götz et al., 2020b). The switchable mirror, consisting of a multilayer stack of 5 nm MoO_x /1 nm Ti / 25 nm Mg / 1 nm Ti / 5 nm Pd, was deposited in a vacuum chamber by electron beam evaporation (VTD, Germany). Areas for the front contact were ablated by laser scribing with a pulsed 532 nm laser after the deposition of the absorber layers to create 16 small 1x1 cm² cells on the 10x10 cm² glass substrate. For optical characterization a demonstrator with 10x10cm² area was fabricated.

The 10x10 cm² glasses with solar cells were introduced together with a bare glass substrate into black aluminum frames to create a double-glazing window. The distance between the two glasses was kept at 10 mm. 3 holes were drilled into the aluminum frame for gas inlet, outlet and to introduce the temperature sensors. The configuration of the system in a double glazing can be seen in Figure 1b. The relevant interfaces are named a1, a2, b1, and b2 (i.e. air - front side of first glass, switchable mirror - air gap, air gap – inside of second glass, outside of second glass – outside air).

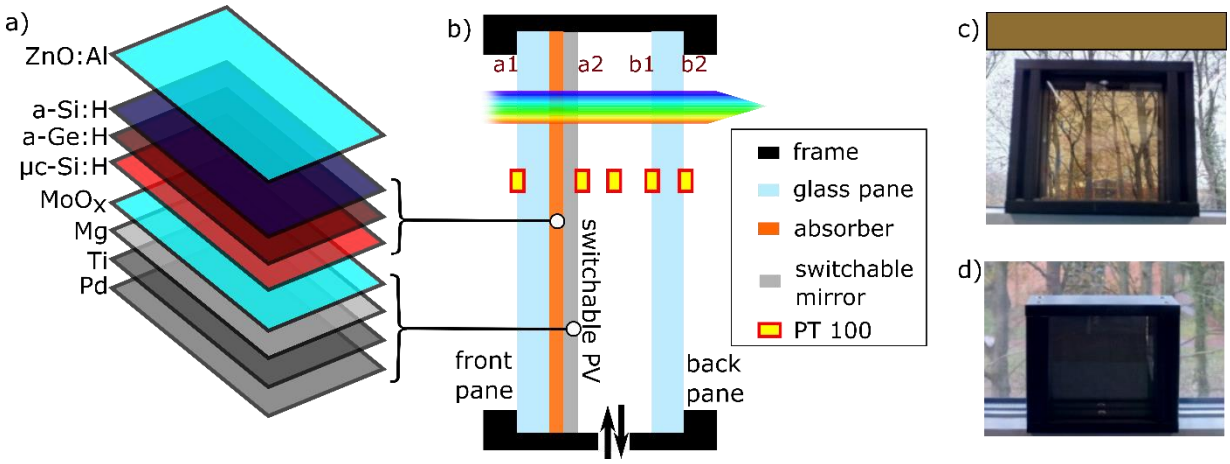

Figure 1. Switchable Photovoltaic Window in Double-Glazing: Layer stack of the switchable solar cell (a); cross-sectional drawing of the double-glazing configuration in LT state (b). Ambient light is transmitted from the left side through the front glass pane which is the substrate for the solar cell layers. The PT 100 temperature sensors are attached for thermal characterization. The interfaces under consideration are named a1 and a2 for the front pane and b1 and b2 for the back pane.

Photography of a demonstrator device of the switchable photovoltaic window in double glazing configuration in LT state together with color patch (c) and in LH state (d) in front of a conventional window.

2.3 Characterization of switchable photovoltaic window

In order to study the performance and electricity generation of a switchable photovoltaic window, criteria have to be defined, which allow for the comparison of the state of a solar cell and the state of a window with glazing elements, as well as the state of a static STPV in the same conditions. Yang et al.(Yang et al., 2019) formulated a process to accurately describe transparent solar cells, which we applied in this study. The transmittance is weighted by the photopic response of the human eye to calculate the average transmittance of visible light. This value is combined with the color rendering index and the color appearance to characterize transparent photovoltaics. Transmission (T) and reflection (R) spectra in the wavelength range between 300 nm and 2500 nm in steps of 1 nm were measured with a Cary 5000 Spectrophotometer (Agilent) equipped with an integrating sphere to account for diffuse and specular light. The absorption was calculated by 1-R-T. The average visible transmittance (AVT), color rendering index (CRI) and the international commission on illumination's (CIE) color space parameters were calculated from the measured data based on the formalism given by Yang et al.(Yang et al., 2019). The emissivity was evaluated by measuring the reflectance and transmittance of the samples in a wavelength range from 2.5 µm to 25 µm in a FTIR spectrometer (Bruker, USA). The emissivity was calculated from the spectral absorptivity in IR with A=1-R, as per Kirchhoff's law of thermal radiation spectral emissivity is equal to absorptivity. Since the transmissivity in the IR range is almost zero between 5 µm and 24 µm wavelength range, as can be seen in the supplementary info Figure S9, we can omit the transmission from this calculation. The spectral emissivity is multiplied with the spectral irradiance of an ideal black body at 300K and integrated over the spectral region from 2.5 to 25 µm, to get the total spectral irradiance value. This integral is divided by the integrated black body spectrum. The solar heat gain coefficient (SHGC) in double glazing configuration is modeled with the software WINDOW7 (v7.8.28.0) using the measured values for T, R and the emissivity as well as glass parameters from the database. The

dimensions of the window were kept similar to the realized small scale device with an area of 10x10 cm^2 and an airgap filled with argon gas of 0.7 cm.

The thermal behavior under AM1.5 G illumination was investigated under a solar simulator (WACOM) where different irradiation intensities were achieved by inserting metal grid filters into the beam path of the light. For the thermal characterization, we used PT100 temperature sensors in 4 wire configurations, connected to a raspberry pi 4 Model B. The position of the sensors in the device can be seen in Figure 1b as well in the photography in Figure 3d. Before the actual measurement, all sensors were calibrated in a water bath with adjustable temperature from 0 to 80 °C. We found the standard deviation of the temperature sensors to be less than 0.5 °C in this temperature range (see also Supplementary Information S3 and S4). For measuring temperature of the double-glazing device under different irradiations, we attached the sensors to the desired surfaces on the device and assured good thermal contact. Sensor which would be subject to direct irradiation were shaded with aluminum foil, to avoid an undesirable increase of temperature. For the measurement we followed the procedure as below:

1. The irradiance was adjusted to a desired value and verified with a calibrated reference solar cell.
2. The solar cell in the double-glazing with attached temperature sensors is placed below the solar simulator with perpendicular incidence of light.
3. The solar cell is kept under constant irradiation until the temperature stabilizes to a constant value.
4. The final temperature values of all elements are extracted by fitting of the temperature vs. time curve (Supplementary S5).

The temperature dependent IV characteristics were measured in a similar way with additional electrical probe contacts attached to the solar cell and connected to a Keithley IV measurement tool.

2.4 Modeling the power output of switchable photovoltaic windows

We used satellite based global irradiation data from the online database PV-GIS for the modelling of the expected electricity generation in different scenarios. The dataset considers the variation of the solar

radiation due to weather, aerosol and climatic conditions. We used the *solar radiation tool* of PV-GIS to get solar radiation data in hourly resolution. We did not use any horizon data, which means that shading from mountains, trees or other nearby buildings was not considered. Typical meteorological year data was used for each region, to avoid extraordinary weather phenomena which would have increased or decreased the output values. Hereby, a typical meteorological month describes each month that is closest to the average in a timescale from 2006 to 2016. The selected year for each month and region can be found in the supporting information (S1). The datasets were adjusted to irradiation on the inclined plane, which is in our case a vertically positioned area (slope=90°), meaning that the SwTPV window is positioned vertically to the surface of the ground. Table 1 describes the input parameters for the PV-GIS interface to generate the datasets. The azimuth orientation describes the cardinal direction the SwTPV is facing. Hereby 0° describe a south facing window, while 90° mean a west facing device and -90° east facing. 180° describe a window facing north.

Table 1: Parameters for PV-GIS datasets

	Agartala	Tunis	Oldenburg
Latitude (decimal degrees)	23.833	36.801	53.151
Longitude (decimal degrees)	91.283	10.192	8.167
Elevation (m)	15	3	7
Solar radiation database	PVGIS-SARAH	PVGIS-SARAH	PVGIS-SARAH
Mounting type	Fixed	Fixed	Fixed
Slope (degrees)	90	90	90
Azimuth (degrees)	from 0 to 180 and to -180 in steps of 22.5 degree	from 0 to 180 and to -180 in steps of 22.5 degree	from 0 to 180 and to -180 in steps of 22.5 degree

The irradiance values in hourly resolution were multiplied with the 2% efficiency of the solar cell to get the power output of the switchable solar window for one hour of the day. Through integration of the power output values over a certain time period, the total power output per day, month or year was calculated.

An algorithm was implemented in Python to study the different switching scenarios. After the import of the irradiation values from PV-GIS into a *pandas* data frame for a given location and orientation of the window, the typical meteorological months are extracted. The model allows to select irradiation data for given time frames, such as working days or weekends. Furthermore, irradiation values can be selected based on a simple threshold to set limits for the switching of the SwTPV form transparent to opaque mode. A flow-chart, describing the algorithm is shown in the supplementary section S8. The irradiance data is given in timesteps of one hour. This implies that the SwTPV is only switched once per hour. This has the advantage that short-time fluctuations in the irradiance, such as a moving cloud are not forcing unnecessary switching events. For the model the switch between LH and LT state is assumed to be instantaneous.

3. RESULTS & DISCUSSION

3.1 Switchable Optical Behavior

To analyze the switchable solar cell in LT and LH state, we studied the optical properties of the cell in a single pane configuration first. A window with switchable transmission and photocurrent generation was fabricated using ultra-thin absorber layers sandwiched between a transparent conductive oxide and a switchable metal mirror. The SwTPV window is fabricated in superstrate configuration, meaning that light passes the glass first before it can be absorbed by the deposited switchable solar cell. For thermal characterization, a double-glazing window was constructed, by placing the switchable solar stack (outer pane) with a float glass (inner pane) into an aluminum frame as can be seen in the cross-sectional view in Figure 1b. The PT100 Thermo sensors were used to study the thermal behavior of the device.

Switching to LT state was initiated by introducing 5% H_2 in N_2 into the double-glazing element for ten minutes. Reverse switching was done by exposure to ambient air. A photography of the window in each state in our lab is shown in Figure 1c and 1d. When the device is in the LT state, light propagates through air into the outer pane of glass (interface a1), through the switchable layer stack – gas interface (a2), the volume of gas in between and then through the inner glass and out of the device (interfaces b1 and b2). Switching of the photovoltaic window is initiated by inserting gas from an inlet also integrated into the frame of the double glazing.

The layer stack of the switchable window is optimized to allow broadband transmission of visible light and reduce any additional coloring effect originating from interference or spectrally selective absorption. The absorbed, transmitted and reflected spectral power intensity from the single switchable solar cell pane in LT and LH state are shown in Figure 2a and 2b. The spectral power intensity is calculated by weighting the measured transmittance, reflectance and calculated absorption with the AM 1.5 G standard solar irradiation spectrum. It can be clearly seen, that the transmitted power decreases drastically switching from LT to LH state. The reflected and absorbed power increase especially for wavelengths larger than 500 nm for the LH state. It is expected that the structure is able to provide good shading due to the high absorption and low transmission in both states. The high absorption in LT state is attributed to parasitic absorption in the switchable mirror layers. This reduces the overall transparency. Since the absorption is high throughout the entire visible spectrum, it appears reasonable to assume that the temperature of the device in the double glazing rises under illumination.

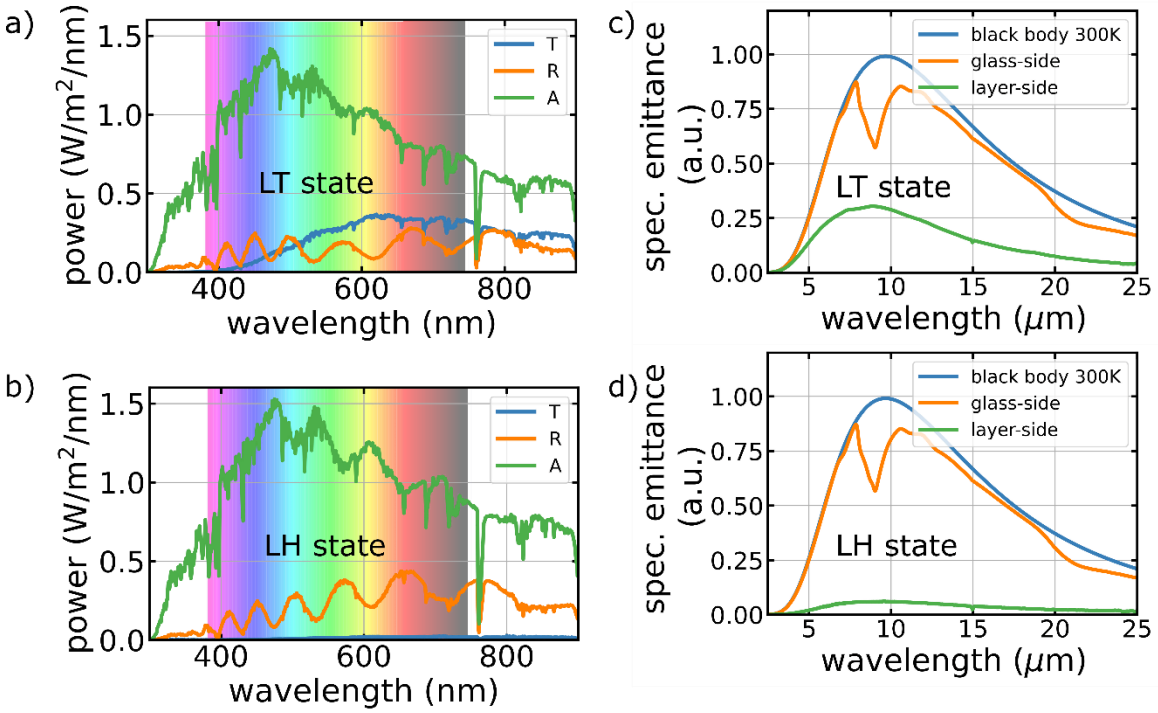

Figure 2. Switchable Optical Behavior: Transmittance (blue), reflectance (orange) and absorption (green) of AM1.5G sun light in LT (a) and LH (b) state of the solar cell. Spectral emittance normalized to the emittance of an ideal black body at 300K (blue) of the device in LT (c) and LH (d) state

The spectra (Figure 2a and a) can also be used to calculate the average visible transmittance (AVT) of the switchable photovoltaic window as well as the color rendering index (CRI). The AVT is calculated as the ratio between transmitted photon flux and the standard AM1.5G incident irradiation convoluted with the photopic response of the human eye. Our aforementioned device as a single pane reaches a value of AVT_{LT}=17.77% in the LT state and an AVT_{LH}=1% in the LH state. For comparison, the bare glass substrate reaches an AVT of 91%. The CRI allows to assess the rendered color fidelity of an object illuminated with light from the transparent solar cell. It has a high impact on the visual comfort inside a room with a switchable photovoltaic window. The single pane device reaches a CRI_{LT}=64.2 in LT state, compared to a bare glass substrate with CRI_{glass}=99.87. The CRI value has to be seen in combination with the CIE color space parameter set, to give full insight into the color fidelity of the device. The achieved

values are L*=49, a*=6.16 and b*=36.31, which corresponds to a point close to color neutrality with a brown tint, also shown in the color patch in Figure 1c.

By measuring the emissivity of each surface of the window we can better understand how IR irradiation contributes to the thermal behavior of the SwTPV in a double glazing as will be discussed later on. Figures 2c and d show the spectral irradiance from the solar cell pane in LT (2c) and LH (2d) state. For details about the calculations refer to the Methods section. In Figure 2d, it can be seen that the glass side of the stack (orange line), which mainly consists of SiO2, has high emission for wavelengths above 2.5 µm and behaves almost like a perfect black body at 300K (blue line). On the solar cell side of the stack, where the outer most layer is the Mg-Ti-Pd switchable mirror, the emissivity is drastically reduced (green line). The metallic layers reflect most of the IR irradiation and only absorb a minor part. While the glass side reaches an emissivity of ε=0.87, the metallic side only has ε=0.06. In the LT state (Figure 2c) it can be seen that the emissivity of the glass-side (orange line) is not affected by the change of Mg to MgH2 and the emissivity remains at ε=0.87. The emissivity of the solar cell layers in LH state on the rear side of the glass increase to ε=0.27. Hence, more IR light can be emitted towards the interior. Interestingly, this shows that the change from LT into LH state not only affects the visible spectral region, but also the IR range. For perpendicular incidence of light, the 10x10 cm² SwTPV in the double-glazing configuration (Figure 1b) shows a solar heat gain coefficient of SHGC=0.103 in LH state and SHGC=0.288 in the LT state. The changing SHGC due to switching of the SwTPV is a consequence of the changing optical parameters. On the one side, it can be deduced that in the LH state, since the emissivity of the solar cell side is low, the SwTPV window would be expected to act as not just UV-VIS but also an IR barrier for hot climates, providing beneficial insulation (Xu and Raman, 2021). On the other side, the low emissivity of the solar cell could help in colder climatic regions to avoid heat loss to the outside of the building when the SwTPV window is integrated into a window with multiple panes as shown in Figure 1b.

3.2 Thermal Behavior of Switchable Photovoltaic Window

After studying the optical behavior of the SwTPV window, it is also relevant to characterize its thermal management. We study the temperature distribution within the device in a double glazing for different irradiation intensities and measure the IV characteristics for varying temperatures. A schematic representation of the cross-section of the window along with the position of the PT100 is shown in Figure 1. The device is positioned below a solar simulator with adjustable irradiation intensities. The details of the measurement can be found in the experimental details and in the Supplementary information S3 to S7. Figure 3a presents the temperature at the selected positions inside and outside the double glazing in in LH state, compared to the irradiance in W/m². The temperature values in transparent state can be found in the supplementary information S6. The temperature rises linearly at all measurement positions with increasing irradiance. It can be seen that the solar cell layers stack has the highest temperature at all irradiation intensities, which is a result of the high local absorption of light. The measured data is transformed into a heatmap in Figure 3b. This enables us to visualize the temperature distribution profile throughout the double glazing. The temperature is significantly reduced adjacent to the SwTPV layers. This is also an indication that the air gap acts as a good insulator between the hot solar cell surface and the second pane. The highest temperature reached under an irradiance of 1018 W/m² is 67 °C, measured on the solar cell layers (interface a2 in Figure 1c). This corresponds to 51 °C at the front surface at interface a1 and 42 °C at the rear surface of the double glazing at interface b2. The measurements show, that the temperature of the complete window is mainly determined by the absorption of light in the solar cell layers and the heat loss mechanisms of the device, especially for high irradiation levels leading to a more pronounced difference in the temperature distribution. The temperature of the remaining sides of the double glazing is influenced by conduction of heat through the glass and the air gap and by convection in the air gap. To study the impact of the temperature on the electrical parameters of the solar cell, we measured the IV-characteristics at different temperatures of the solar cell layers at interface a2. We used a constant irradiation of 1000 W/m² for this experiment. The results can be seen in Figure 3c. The corresponding IV curves can be found in the supplementary information S7. It is well-know that a rise

of temperature reduces the band gap energy required for bond breaking and carrier photogeneration. These changes in the optoelectronic properties of the semiconductor materials induces an alteration in the solar cell devices output characteristics (Dupré et al., 2017). The open circuit voltage (V_{oc}) decreases steadily by increasing temperature with a temperature coefficient of -2.3 mV/K, following a linear behavior. This corresponds to a decrease of 0.5 %/K, which is similar to the coefficient found for polycrystalline Silicon based semi-transparent PV modules of 0.49 %/K (Park et al., 2010), due to the similarity in the energy bandgap between both the amorphous germanium nano-absorber (Meddeb et al., 2020) and the polycrystalline Si absorber. The short circuit current (J_{sc}) increases for higher temperatures, as the lower associated optical bandgap could enlarge the portion of photon energies capable of electron-hole pair generation (Dupré et al., 2017). This might also be attributed to the promoted contribution of the currents generated by thermionic emission process in the ultrathin quantum well p-i-n configuration (Meddeb et al., 2020). The thermal coefficient for the J_{sc} is given by 0.013 mA/cm²/K. The power at the maximum power point (P_{mmp}) stays almost constant from 27 °C to 40 °C and starts slowly decreasing thereafter. This means that the efficiency of the device is almost constant for a broad temperature range, which might be explained by the counterbalance trend where the voltage lowering magnitude overcomes the rise of the photocurrent. At 54 °C the P_{mpp} reaches 95.7% of the P_{mpp} at 30 °C. The cyclability of the SwTPV device is a critical issue. It was already shown that the device is able to undergo several switching cycles (Götz et al., 2020a) but further improvement is needed. While the gasochromic Mg layer is able to be switched multiple times without a significant change of optical properties(Tajima et al., 2008), the absorber layers experience shunting leading to the electrical degradation of the solar cell.

Overall, this thermal behavior analysis shows several important points. The solar cell layer stack at interface a2 can reach high temperatures up to 67°C for irradiation of 1018 W/m². The interior of the building is shielded by the double glazing from the high temperatures by the airgap between first and second pane. Since 1018 W/m² corresponds to the AM1.5G spectrum this might be in most cases the highest irradiation received by the window. In a real application scenario, the SwTPV would be

positioned vertically and not horizontally as is the case for this experiment. Therefore, the gaseous interior in the gap between the windows would experience a temperature gradient from top to bottom as is the case for double glazings in general (De Giorgi et al., 2011). This would also lead to a slightly different temperature distribution of the solar cell layers with the highest temperature at the top of the device.

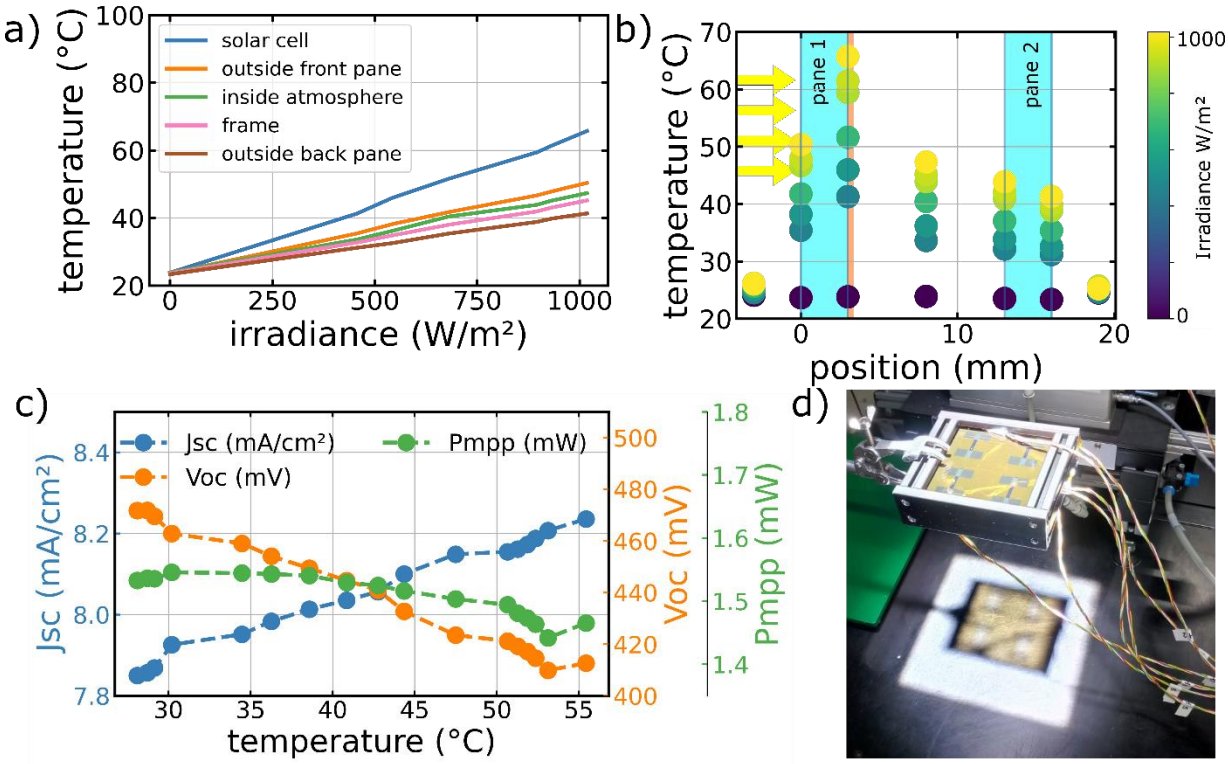

Figure 3. Thermal Behavior of Switchable Photovoltaic Window: Temperature of elements of the double glazing depending on irradiance (A); Temperature distribution inside the double glazing for different values of irradiance (B); Temperature dependence of shorth circuit current (Jsc), open circuit voltage (Voc) and maximum power point (Pmpp) (C); Photography of the measurement setup under illumination (D).

The temperature dependent IV measurements (Figure 3c and supplementary information S7) showed, that the overall efficiency is not drastically reduced by these temperatures and therefore a constant efficiency and a robust thermal insensitivity can be assumed independent of the temperature for most applications.

The studied SwTPV reaches a PCE of 1.55% in LH state while no efficiency is measured in the transparent state. The IV curves for different temperatures are shown in the supplementary section S7. The PCE is similar to other switchable PV technologies. Huaulmé et al. (Huaulmé et al., 2020) reached a PCE between 1.4% and 4.2% for a photochromic dye sensitized solar cell. Kwon et al. (Kwon et al., 2015) demonstrated a combination of dye sensitized solar cell with a liquid crystal switchable layer with efficiencies from 1.1% to 3.2%. A champion solar cell from a device similar to the here presented reached an efficiency of 2.0% (Götz-Köhler et al., 2021).

3.3 Power Generation Model

After studying the optical and thermal behavior of the switchable photovoltaic window, we want to assess the power generation potential in generic application scenarios. We use PV-GIS satellite-based irradiation and weather data for different regions in the northern hemisphere in a typical meteorological year adjusted for each region. We consider photovoltaic windows with 1 m² area and 2% PCE facing all cardinal directions. The SwTPV windows are positioned vertically in an imaginary façade and are controlled by different switching models. The locations, where we study the SwTPV window performance, are chosen in such a way that they represent different climatic regions of the northern hemisphere. Figure 4b shows the locations of the studied regions. We first consider the city of Agartala in India (blue arrow) with a humid tropical climate. It experiences hot and humid summers followed by monsoon season, while the winters are dry and comparably mild. The summer lasts from April to October while winter lasts from November to March. Tunis in Tunisia (orange arrow) is the second region featuring a Mediterranean climate and is characterized by dry and hot summers and mild winters with moderate rainfall. The last location in our study is Oldenburg, Germany (green arrow) with a moderate oceanic climate where summers are mild and only last from beginning of June to end of August. Especially interesting is here that Oldenburg has dark winters with only few hours of sunshine. Overall the climate is dominated by frequent rainfall distributed over the whole year.

3.4 Irradiation Profiles of Different Climatic Regions

Figure 4a shows the solar irradiance profiles on south facing windows in Agartala, Tunis and Oldenburg. The elevation of the sun throughout the day determines the amount of irradiance that the solar window receives. The azimuth orientation of the SwTPV window determines the time during which the majority of irradiance is received. The comparison plots for different cardinal directions can be found in the supporting information S2-1, S2-2 and S2-3. Windows facing east/west see rather the morning/evening sun, while windows facing south receive more sunlight throughout the entire day. Windows facing north receive the lowest irradiation. The cloud and rain coverage at a certain location can change during the day and develop repeating schemes meaning the solar irradiation on the windows facing east and west may not be symmetrical. For example, rainfall in the evening might happen more often than in the morning thus leading to different irradiation on east and west facing windows during the course of a year. The figure presents the rolling seven-day average of the sum (*G(i)*) of direct (*Gb(i)*) and diffuse (*Gd(i)*) irradiation on the inclined plane of the photovoltaic windows.

$$G(i) = Gb(i) + Gd(i)$$

Several distinct differences emerge in the irradiation profiles of the three locations throughout a typical meteorological year in the respective region. In Agartala and in Tunis, the sun rises high up in the sky (reaching maximum elevation= 89.6° for Agartala, reaching max elevation =76.63° for Tunis) during the months from April to August, leading to comparable low direct irradiation onto the south facing window during this time. On the other side, in Oldenburg the sun only reaches a maximum elevation of 60.3°, leading to more direct irradiation onto the photovoltaic window in the months between April and August. Furthermore, the weather plays - like for every other solar cell technology - an important role, as clouds, fog and rain reduce the direct irradiation and negatively influence the performance of the photovoltaic windows. It is worth noting, that the fluctuation of the daily irradiance, seen by the standard deviations of the rolling average in Figure 4a, is very high in Oldenburg, compared to the other cities. This is especially remarkable during the months between April and September, where Agartala and Tunis have

long periods of homogeneous weather and the irradiance does not vary within a time period of several days. The uncertainty of the weather conditions throughout the entire year influences the amount of switching performed by the SwTPV window.

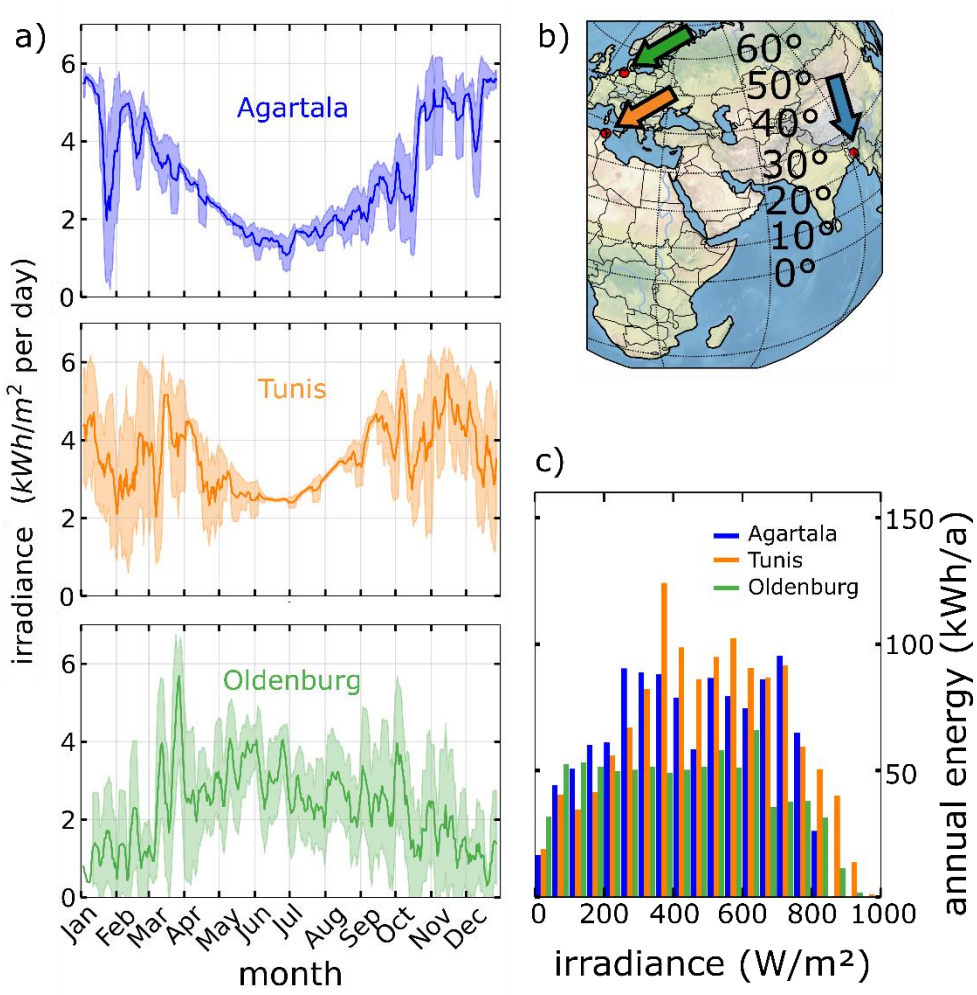

Figure 4. Irradiation Profiles on Vertically Inclined Plane in Different Climatic Regions: Irradiance in seven-day rolling average with standard deviation during a typical meteorological year on south facing windows in Agartala (India), Tunis (Tunisia) and Oldenburg (Germany) (a). Locations of the regions under consideration (b). Annually received energy on 1m² area of a south facing window depending on the irradiation power (c).

Figure 4c shows a histogram of the received annual energy of a south facing window in dependence on the momentary irradiation power over a complete year in the three cities under consideration. The

irradiation is sorted into 50 W/m^2 bins and the values of each bin are summed up to calculate the annual energy in the respective irradiance power range. In the city of Oldenburg (green), the received energy is distributed equally over all irradiance powers. For a majority of time, the sunlight incidence on the window has only low power, while high power irradiation only occurs for short time, as can also be seen in Figure 4a. This leads to the homogeneous distribution of the received annual energy. A completely different result can be observed in Tunis, where the most energy per year is received from irradiation with a power between 350 and 400 W/m². Up to powers of 750 W/m², the received energy per year remains high. Agartala shows an even steeper increase of annual energy with increasing irradiance, but does not reach the individual high energy values of Tunis. The received energy in Agartala remains relatively constant between 350 and 750 W/m². The observation of this energy distribution is helpful for the next step of defining a switching model, where a cut-off value for incoming irradiance has to be defined.

3.5 **Threshold Switching in Different Climate Zones**

To study the amount of generated electricity during an entire year by a switchable photovoltaic window, a suitable model has to be defined, which describes the conditions when the window is switched into LT mode or into LH mode. We assume a constant power conversion efficiency of 2%. The reduction of efficiency due to temperature effects was omitted since the experiments above showed only minor dependence of the efficiency on the device temperature. We first define a threshold switching model. This model assumes, that above a certain threshold value of irradiance the window is in LH mode to generate electricity. When the irradiance lays below the threshold, the window is switched into the LT state.

$$PVstate\big(G(i)\big) = \begin{cases} LT, & if\ G(i) \le I_0 \\ LH, & if\ G(i) > I_0 \end{cases}, with\ 0 \le I_0 \le 1000\frac{W}{m^2}$$

Hereby, I_0 is the threshold value for the irradiance on the inclined plane ($G(i)$). This threshold can be adjusted to maximize personal comfort within the building, or to maximize energy generation. For

example, it can be set to a specific value to prevent direct sunlight from disturbing the view on a desktop monitor in an office environment and reduce the heat flux into the building on days with high solar irradiance.

Figures 5a to c demonstrate the energy output in a typical meteorological year for the three cities discussed above, depending on the varying threshold value I_0 for hourly irradiance values. All three cities show different results depending on their different irradiation profiles. In Agartala and Oldenburg, the south facing SwTPV device reaches the highest energy generation for almost all threshold values. In Tunis, windows facing east-south-east or west-south-west have a higher generation potential for threshold values above $I_0 = 400$ W/m². The highest power generation in all three cities is reached for a threshold of 0 W/m², corresponding to a SwTPV always being set to LH state. When the threshold value is increased, the annual electricity generation is reduced. This is due to the fact that the solar cell is operated less often and the device is kept in LT mode for longer time. It becomes apparent from the contour plots that SwTPV windows in Tunis are able to reach higher power generation than in Agartala. Oldenburg shows the lowest potential for electricity generation with SwTPV in this threshold model.

Every curve reaches a point, where the energy generation is reduced to zero for all directions due to the level of the threshold value. This is the upper limit for the threshold, corresponding to a SwTPV window always set to LT state. The zero-power generation point depends on the irradiance on the window compared to the threshold point. This point is reached in all cities at a threshold value of around $I_0 = 800$ W/m². Almost no irradiation above this intensity reaches the window due to its vertical position. This can also be seen in the histogram in Figure 4c, where the irradiation energy for irradiation above 800 W/m² decreases steeply.

It can also be seen that the distribution of power generation is not completely symmetric between east and west facing SwTPV. While Agartala and Tunis show higher generation potential for windows facing

more towards west compared to the eastern orientation, Oldenburg has a slightly higher potential for the eastern direction.

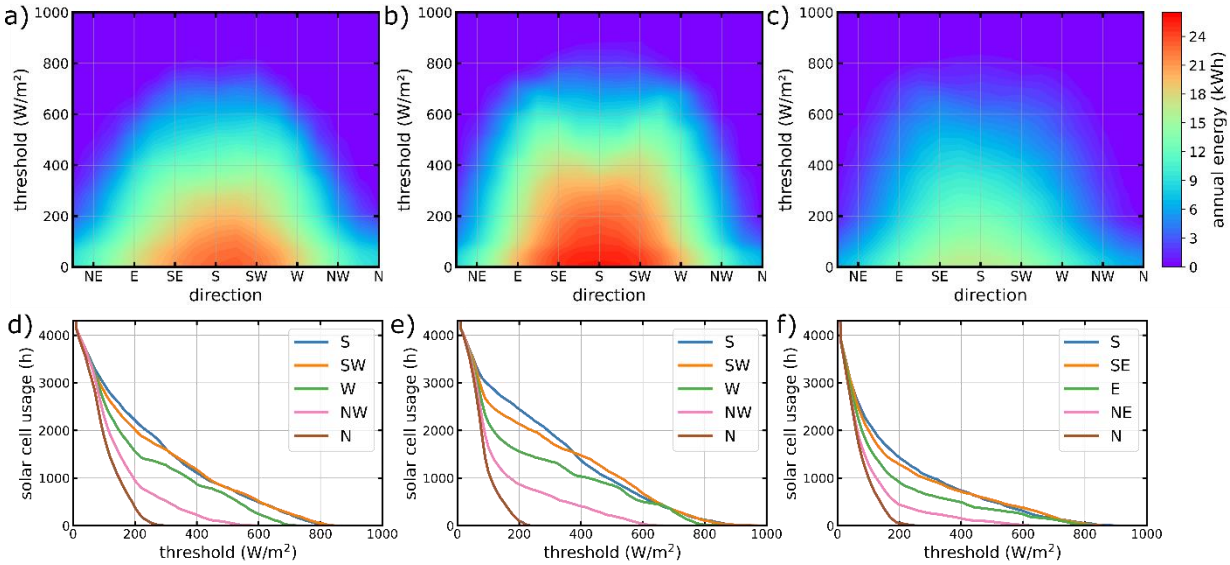

Figure 5. Threshold Switching in Different Climate Zones: Annual energy generation of 1m² SwTPV window versus threshold for incident solar irradiation for different cardinal direction in Agartala (a), Tunis (b) and Oldenburg (c). Total time in hours the photovoltaic window is operated in LH state and generates electricity versus threshold for incident solar irradiation in Agartala (d), Tunis (e) and Oldenburg (f).

To further study the usage of the threshold model, we also analyzed the total hours per year during which the photovoltaic window is in LH mode (Figure5 d to f) and generates electricity. The figures show a histogram of the distribution of irradiance for five orientations of the window. We chose for each city the east/west directions with higher generation potential, meaning for Agartala and Tunis the west facing windows and for Oldenburg east facing. A drastic reduction of the solar cell usage time can be observed, when the threshold value is increased from zero to 200 W/m². For higher threshold values, the decrease in the solar cell usage time is rather gradual. The steep drop in the beginning results from the large amount of time at dusk and dawn, where only very low irradiation incidence on the SwTPV window or from days with high cloud coverage. The comparison between usage time and annual power output shows that high irradiation is more important for the power output, than long timeframes with low irradiation. This

result is a direct consequence of the distribution of annual received energy vs irradiance in Figure 4d. This fits perfectly to the requirements of the SwTPV window to prevent light from entering the room, when it would lead to an increase in heat or disturb the visual comfort of the occupant, which is more likely to happen at high irradiation powers. In the model shown here, switching is only done at a maximum frequency of once per hour. Using irradiation data with higher temporal resolution would also require higher switching frequencies to map the short time changes such as partial cloud coverage to the electricity generation. Therefore, also the switching speed would have to be adapted.

3.6 Power Generation Model for Switchable Photovoltaic Window

The analysis of irradiance and the usage time for different switching thresholds at various locations shows that SwTPV windows have to be carefully adjusted to the momentary irradiance, but also to the annual energy distribution. To study the expected power generation in a realistic scenario, two models are analyzed. First, we look at an office building, occupied with employees on weekdays from 9 am until 5 pm. During this time, the windows will be transparent and only switch into the absorptive state, when the irradiance surpasses a threshold value of 550 W/m². This value is chosen since it allows high usage time of the solar cell, while allowing the switchable window to be in transparent state sufficiently often. During the weekends (Saturday – Sunday), the office is unoccupied and there is no requirement of indoor lightning and hence no irradiance threshold is defined. The SwTPV window is set to LH mode to generate electricity during this time. The annual power output for this scenario is shown in Figure 6a. An office building in Tunis reaches the highest power output (12-16 kWh/m² per year) for directions facing south-east and south-west with a maximum for the south-western orientation. A SwTPV device in this scenario in Oldenburg produces only up to 8 kWh/m² of electricity per year. A SwTPV window in Agartala has the second-best performance for all directions reaching values that are close to those of Tunis especially in the south-south-eastern direction.

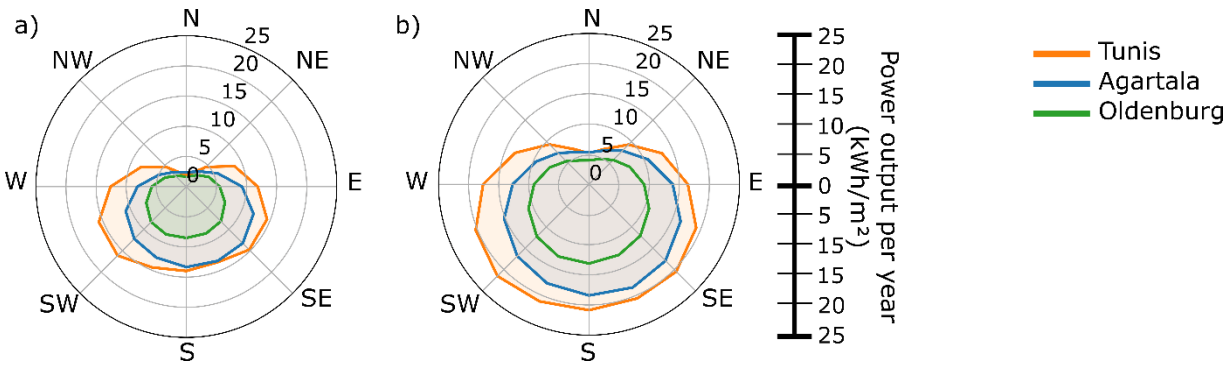

Figure 6. Power Generation Model for Switchable Photovoltaic Windows: Power output in one year per meter square for a switchable photovoltaic window modeled for an office building facing different directions (a). Power output for residential buildings (b).

In this scenario, the threshold switching is used for five out of seven days per week, while the solar cell state is only constantly used during the weekend. The power output is therefore dominated by the threshold switching and the irradiance during weekends. For windows facing north, this means that almost no electricity is generated throughout the year. The power output follows mainly the results from Figure 5.

The second scenario is adapted to residential areas, such as apartments or houses or even hotel rooms. Here, the windows are set to LH mode during weekdays from 9 am to 5 pm, when the residents are at work and the rooms are generally unoccupied. During the weekend, the windows are set to transparent state and only switch into tinted mode, when the irradiance exceeds the threshold value of 550 W/m². The results are shown in Figure 6b. Here, the switchable window in Tunis is able to generate above 20 kWh/m² per year, when facing in south direction. This is significantly more than the windows in the office scenario would generate. The reason for this result is the higher usage time during weekdays, where the window is set to be in tinted state for most of the time due to inoccupancy of the room. the minimal usage of the threshold model (only on during weekends) increases the total electricity generation of the device. This shows, that a predefined schedule for longtime switching into the LH state are more beneficial than just using a simple threshold model. Overall, the results show that the annual power output for switchable photovoltaic windows depends strongly on the climatic region where they are installed in.

Tunis, which is located at the Mediterranean Sea provides the best climatic conditions together with high irradiation for the switchable photovoltaic window compared to the other two cities.

To compare the results of the modeling study in a larger context, PV technology which can be applied or integrated into a building has to be included in our consideration. Roof-top PV has shown to reach specific yields over 1000kWh per installed peak capacity in kilowatts in Germany over the last ten years (kWh/kW_p) (Schardt and te Heesen, 2021). The technology presented here would allow for a yield of 65 kWh/kW_p in Oldenburg, 110 kWh/kW_p in Tunis and 90 kWh/kW_p in Agartala considering south facing SwTPV devices based on the presented residential switching scenario. BIPV modules in the façade can be treated similarly to the SwTPV devices concerning their received irradiance, but as opaque elements generally show higher efficiencies. In general, SwTPV can only supply a significant part to the total energy generation, if it is applied to a large area. This is especially the case in large modern buildings with large WWR, where the area for standard opaque BIPV is limited by the façade area and roof-top PV cannot be applied due to cooling systems or architectural structures occupying the roof. In this case SwTPV are a promising way to generate electricity without allocation of a dedicated area for opaque PV, which was also shown for semitransparent PV in a recent publication by Panagiotidou et al. (Panagiotidou et al., 2021).

The usage of a switchable photovoltaic window would also increase the energy consumption for additional illumination due to its reduced transparency in residential and office scenarios. It was shown by Miyazaki et al. (Miyazaki et al., 2005) that for STPV the electric illumination has to be coupled to the natural illumination to increase the benefit of the photovoltaic window. It does raise a concern that in darker climates and season the switching could be done only seasonal when light and heat is given preference over power generation. Overall, the efficiency of the device must be further increased in order to be considered for commercial application.

For the city of Agartala which is located in a tropical climate region, the applications would vary compared to the scenario discussed above. In the hot seasons, SwTPV could be used to reduce heat influx

and therefore reduce the energy consumption of heating, ventilation and air conditioning (HVAC) systems. Hereby, the electricity generation of the switchable photovoltaic window would additionally allow for assistance in the illumination and electrical cooling devices. During the monsoon season, the irradiance on the photovoltaic windows is reduced, which can also be seen in Figure 4a. Here the switchable photovoltaic windows would only play a minor role in the electricity generation, compared to the rest of the year.

In Tunis, the Mediterranean climate allows for high electricity generation throughout the entire year. Here, the switchable photovoltaic window generates the highest power per year in all scenarios compared to the other two cities. It can serve both purposes, the reduction of heat influx through adaptive shading as well as the generation of up to 22 kWh/m² per year. It is noteworthy that the corresponding electricity consumption per capita in Tunisia is 1,520 kWh, which is significantly less than in Europe (Enerdata). This shows, that in Tunisia the benefits of SwTPV are higher than in countries further up in the north. During the course of the day, the window would prevent the house from heating up too much, while it also allows natural illumination in the morning and in the evening. This could help to reduce the power consumption of air-conditioners. Hereby, the electrical output of the SwTPV device would only supply a minor part of the required electricity, since conventional air-conditioner systems use several hundreds of kilowatt hours per year. The influence of the electricity generation and the dynamic shading on supporting air-conditioners and HVAC systems in general will be the subject of further studies.

An implementation of the SwTPV in a real building could replace conventional windows. With a central gas supply for the switching gases (diluted hydrogen and pressured dry air) and a connection to the in-house electricity grid this type of windows would be preferably installed in new buildings during the construction. The cost of installation would be reduced by the fact that the SwTPV could replace expensive low emissivity windows and additional mechanical shades and would not require further installations like façade mounted BIPV. Furthermore, the active control over the SwTPV state leads to energy savings compared to static semi-transparent PV (Favoino et al., 2016). The switching could be

initiated as described above by external factors such as local irradiance or a given time, or through a switching command by the resident. Further research will show how the economic feasibility of the SwTPV technology can be treated and what efficiencies have to be reached to become a realistic option for the integration into buildings. Further models can also be developed to approach a more realistic application scenario. For example, the simulation of a switching process which guarantees constant illumination inside the building throughout the day.

Taking all these considerations into account it can be stated that switchable photovoltaic windows would be more valuable in Mediterranean and sub-tropical to tropical regions. Tunis and Agartala both appear to be suitable locations for using a threshold model, since the irradiance remains high over most of the year. For places located in higher latitudes such as Oldenburg, the threshold value would have to be adjusted for each season to increase the benefit of the switchable window.

4. CONCLUSION

Switchable transparent photovoltaics are drawing great attention in the building integrated PV community because of the possibility to replace conventional windows. This would open up a completely new area on the building envelope for electricity generation. The aim of the study was to evaluate the performance of a switchable photovoltaic window integrated into a double-glazing system. We prove that both, the transmission and the emissivity of the SwTPV window can be dynamically switched. The analysis of the thermal behavior of the device under varied irradiance in laboratory conditions showed that the double glazing effectively shields the transfer of heat from the solar cell to the indoor. Furthermore, the electrical performance of the solar cell is affected by the temperature only in a minor way. Since the temperature of all parts of the glazing is influenced by the high temperature of the solar cell layer, a triple glazing could further reduce the impact of heat conduction by adding a second air gap. Taking into consideration the aforementioned criteria, a power generation model using satellite-based irradiance data for the integration of SwTPV technology in real scenarios was established, including irradiation profiles and threshold switching cases of different climatic regions, as well as various window

orientations. It is shown that the sub-tropic and Mediterranean regions of the earth provide more potential for switchable electricity generation than locations at higher latitude, as was expected. Especially the ability to provide smart shading might be useful in Mediterranean and sub-tropical regions where the heat flux into the building could be reduced and at the same time solar energy would be converted to electricity. While this study set out to find the base scenario for a switchable photovoltaic technology and its application, the findings can also be extended to other smart PV window technologies. The results indicate, that switchable photovoltaic windows can be a valuable addition to buildings for smart shading and electricity generation in the future.

DECLARATION OF INTERESTS

The authors declare that they have no known competing financial interests or personal relationships that could have appeared to influence the work reported un this paper.

AUTHOR CONTRIBUTIONS

Conceptualization, M.G.-K.; methodology, M.G.-K., U.B., D.B. and H.M.; investigation, M.G.-K., U.B.; writing – original draft, M.G.-K.; writing – review & editing, M.G.-K., U.B., H.M., K.G., N.N., D.B. and M.V. ; validation, M.G.-K., U.B., H.M.; formal analysis, M.G.-K., U.B., H.M; visualization, M.G.-K., N.N.; software M.G.-K., N.N., U.B.; resources, M.V., C.A..; data curation, M.G-K., K.G., M.V., C.A.; supervision, K.G., M.V., C.A.; project administration, K.G., M.V., C.A.; funding acquisition, K.G., M.V., C.A.

ACKNOWLEDGEMENTS

The authors would like to thank C. Lattyak, N. Osterthun, P. Schwager and O. Sergeev for important and fruitful discussions. The authors also would like to thank C. Koch and S. Schlüters for helpful ideas and discussions concerning the temperature measurements.

APPENDIX: SUPPLEMENTARY INFORMATION

Supplementary Information, Table S1, Figures S2-S9

Table S1: selected typical meteorological year for each month and location of the PV-GIS dataset; Figure S2-1: Irradiance during a typical meteorological year in Agartala, India; Figure S2-2: Irradiance during a typical meteorological year in Tunis, Tunisia; Figure S2-3: Irradiance during a typical meteorological year in Oldenburg, Germany; Figure S3: Calibration of temperature sensors; Figure S4: temperature uniformity calibration of PT 100 sensors; Figure S5: Equilibrium temperature fits; Figure S6: Temperature distribution of double-glazing in LT state; Figure S7: IV curves of temperature dependent IV measurement of switchable PV in LH state; Figure S8: Flow chart describing the Python algorithm; Figure S9: Transmission spectra from FTIR measurements of SwTPV in LH and LT state

REFERENCES

Asfour, O., 2018. Solar and Shading Potential of Different Configurations of Building Integrated Photovoltaics Used as Shading Devices Considering Hot Climatic Conditions. Sustainability 10(12), 4373.

Cannavale, A., Manca, M., De Marco, L., Grisorio, R., Carallo, S., Suranna, G.P., Gigli, G., 2014. Photovoltachromic device with a micropatterned bifunctional counter electrode. ACS applied materials & interfaces 6(4), 2415-2422.

De Giorgi, L., Bertola, V., Cafaro, E., 2011. Thermal convection in double glazed windows with structured gap. Energy and Buildings 43(8), 2034-2038.

Dupré, O., Vaillon, R., Green, M.A., 2017. Temperature Coefficients of Photovoltaic Devices, Thermal Behavior of Photovoltaic Devices. pp. 29-74.

Dussault, J.-M., Gosselin, L., 2017. Office buildings with electrochromic windows: A sensitivity analysis of design parameters on energy performance, and thermal and visual comfort. Energy and Buildings 153, 50-62.

Enerdata, Tunisia Energy Information. https://www.enerdata.net/estore/energy-market/tunisia/. (Accessed 19.08.2021 2021).

Favoino, F., Fiorito, F., Cannavale, A., Ranzi, G., Overend, M., 2016. Optimal control and performance of photovoltachromic switchable glazing for building integration in temperate climates. Applied Energy 178, 943-961.

Fiorito, F., Cannavale, A., Santamouris, M., 2020. Development, testing and evaluation of energy savings potentials of photovoltachromic windows in office buildings. A perspective study for Australian climates. Solar Energy 205, 358-371.

Fung, T.Y.Y., Yang, H., 2008. Study on thermal performance of semi-transparent building-integrated photovoltaic glazings. Energy and Buildings 40(3), 341-350.

Götz-Köhler, M., Meddeb, H., Gehrke, K., Vehse, M., Agert, C., 2021. Ultrathin Solar Cell With Magnesium-Based Optical Switching for Window Applications. IEEE Journal of Photovoltaics, 1-7.

Götz, M., Lengert, M., Osterthun, N., Gehrke, K., Vehse, M., Agert, C., 2020a. Switchable Photocurrent Generation in an Ultrathin Resonant Cavity Solar Cell. ACS Photonics 7(4), 1022-1029.

Götz, M., Osterthun, N., Gehrke, K., Vehse, M., Agert, C., 2020b. Ultrathin Nano-Absorbers in Photovoltaics: Prospects and Innovative Applications. Coatings 10(3), 218.

Huaulmé, Q., Mwalukuku, V.M., Joly, D., Liotier, J., Kervella, Y., Maldivi, P., Narbey, S., Oswald, F., Riquelme, A.J., Anta, J.A., Demadrille, R., 2020. Photochromic dye-sensitized solar cells with light-driven adjustable optical transmission and power conversion efficiency. Nat Energy 5(6), 468-477.

Huld, T., Müller, R., Gambardella, A., 2012. A new solar radiation database for estimating PV performance in Europe and Africa. Solar Energy 86(6), 1803-1815.

Ke, Y., Chen, J., Lin, G., Wang, S., Zhou, Y., Yin, J., Lee, P.S., Long, Y., 2019. Smart Windows: Electro-, Thermo-, Mechano-, Photochromics, and Beyond. Adv Energy Mater 9(39), 1902066.

Kwon, H.K., Lee, K.T., Hur, K., Moon, S.H., Quasim, M.M., Wilkinson, T.D., Han, J.Y., Ko, H., Han, I.K., Park, B., Min, B.K., Ju, B.K., Morris, S.M., Friend, R.H., Ko, D.H., 2015. Optically Switchable Smart Windows with Integrated Photovoltaic Devices. Adv Energy Mater 5(3), 1401347.

Lee, K., Um, H.-D., Choi, D., Park, J., Kim, N., Kim, H., Seo, K., 2020. The Development of Transparent Photovoltaics. Cell Reports Physical Science, 100143.

Liao, W., Xu, S., 2015. Energy performance comparison among see-through amorphous-silicon PV (photovoltaic) glazings and traditional glazings under different architectural conditions in China. Energy 83, 267-275.

Lin, J., Lai, M., Dou, L., Kley, C.S., Chen, H., Peng, F., Sun, J., Lu, D., Hawks, S.A., Xie, C., Cui, F., Alivisatos, A.P., Limmer, D.T., Yang, P., 2018. Thermochromic halide perovskite solar cells. Nature materials 17(3), 261-267.

Ling, H., Wu, J., Su, F., Tian, Y., Liu, Y.J., 2021. Automatic light-adjusting electrochromic device powered by perovskite solar cell. Nature communications 12(1), 1010.

Lunt, R.R., 2012. Theoretical limits for visibly transparent photovoltaics. Appl Phys Lett 101(4), 043902.

Martín-Chivelet, N., Guillén, C., Trigo, J., Herrero, J., Pérez, J., Chenlo, F., 2018. Comparative Performance of Semi-Transparent PV Modules and Electrochromic Windows for Improving Energy Efficiency in Buildings. Energies 11(6).

Meddeb, H., Osterthun, N., Götz, M., Sergeev, O., Gehrke, K., Vehse, M., Agert, C., 2020. Quantum confinement-tunable solar cell based on ultrathin amorphous germanium. Nano Energy 76, 105048.

Miyazaki, T., Akisawa, A., Kashiwagi, T., 2005. Energy savings of office buildings by the use of semi-transparent solar cells for windows. Renewable Energy 30(3), 281-304.

Murray, J., Ma, D.K., Munday, J.N., 2017. Electrically Controllable Light Trapping for Self-Powered Switchable Solar Windows. Acs Photonics 4(1), 1-7.

Panagiotidou, M., Brito, M.C., Hamza, K., Jasieniak, J.J., Zhou, J., 2021. Prospects of photovoltaic rooftops, walls and windows at a city to building scale. Solar Energy 230, 675-687.

Park, K.E., Kang, G.H., Kim, H.I., Yu, G.J., Kim, J.T., 2010. Analysis of thermal and electrical performance of semi-transparent photovoltaic (PV) module. Energy 35(6), 2681-2687.

Peng, J., Curcija, D.C., Lu, L., Selkowitz, S.E., Yang, H., Zhang, W., 2016. Numerical investigation of the energy saving potential of a semi-transparent photovoltaic double-skin facade in a cool-summer Mediterranean climate. Applied Energy 165, 345-356.

Peng, J., Lu, L., Yang, H., Ma, T., 2015. Comparative study of the thermal and power performances of a semi-transparent photovoltaic façade under different ventilation modes. Applied Energy 138, 572-583.

Schardt, J., te Heesen, H., 2021. Performance of roof-top PV systems in selected European countries from 2012 to 2019. Solar Energy 217, 235-244.

Skandalos, N., Karamanis, D., 2016. Investigation of thermal performance of semi-transparent PV technologies. Energy and Buildings 124, 19-34.

Steenhoff, V., Theuring, M., Vehse, M., von Maydell, K., Agert, C., 2015. Ultrathin Resonant-Cavity-Enhanced Solar Cells with Amorphous Germanium Absorbers. Advanced Optical Materials 3(2), 182-186.

Šúri, M., Huld, T.A., Dunlop, E.D., 2005. PV-GIS: a web-based solar radiation database for the calculation of PV potential in Europe. International Journal of Sustainable Energy 24(2), 55-67.

Tajima, K., Yamada, Y., Bao, S., Okada, M., Yoshimura, K., 2008. Near colorless all-solid-state switchable mirror based on magnesium-titanium thin film. J Appl Phys 103(1), 013512.

Traverse, C.J., Pandey, R., Barr, M.C., Lunt, R.R., 2017. Emergence of highly transparent photovoltaics for distributed applications. Nat Energy 2, 849-860.

Wheeler, L.M., Moore, D.T., Ihly, R., Stanton, N.J., Miller, E.M., Tenent, R.C., Blackburn, J.L., Neale, N.R., 2017. Switchable photovoltaic windows enabled by reversible photothermal complex dissociation from methylammonium lead iodide. Nature communications 8(1), 1722.

Wu, J.J., Hsieh, M.D., Liao, W.P., Wu, W.T., Chen, J.S., 2009. Fast-switching photovoltachromic cells with tunable transmittance. ACS Nano 3(8), 2297-2303.

Xu, J., Raman, A.P., 2021. Controlling radiative heat flows in interior spaces to improve heating and cooling efficiency. iScience 24(8), 102825.

Yang, C., Liu, D., Bates, M., Barr, M.C., Lunt, R.R., 2019. How to Accurately Report Transparent Solar Cells. Joule 3(8), 1803-1809.

Yao, M., Li, T., Long, Y., Shen, P., Wang, G., Li, C., Liu, J., Guo, W., Wang, Y., Shen, L., Zhan, X., 2020. Color and transparency-switchable semitransparent polymer solar cells towards smart windows. Science Bulletin 65(3), 217-224.